

# Minimal conditions for vasomotion

Jaijus Pallippadan Johny\* and Tim David†

Bluefern Supercomputing Unit

University of Canterbury

Christchurch, New Zealand

\*jaijus.pallippadanjohny@pg.canterbury.ac.nz

†tim.david@canterbury.ac.nz

**Abstract**—The occlusion of arteries during ischaemia causes a state of insufficient blood supply and hypoperfusion in downstream to keep the brain functioning. Hypoperfusion in human brain is a critical event which leads to cerebral hypoxia with high risk of developing impairment. Vasomotion can be induced in the above situation of reduced perfusion. This might increase the blood flow by decreasing the effective vascular resistance and lead to enhanced perfusion. Therefore, one could assume that vasomotion is a regulating mechanism associated with hypoperfusion to control vascular resistance, blood flow and tissue perfusion. It is therefore important to explore the underlying mechanisms and the factors affecting the initiation and spread of vasomotion. In future, this study will help the early diagnosis and treatment of previously mentioned pathological conditions. This study analyses the minimum condition required to initiate vasomotion. It is shown that a minimum number of cells need to be stimulated with sufficient amount of depolarization to initiate conduction of contraction.

## I. INTRODUCTION

Vasomotion is synchronized oscillations of vascular tone which occur in many vascular networks such as in the human brain. It is initiated locally by metabolic stresses and spreads over several millimetres of the vessel. Physiological functions of vasomotion are not fully understood. However, one of such implication is that it can enhance tissue oxygenation when perfusion is limited (Tsai and Intaglietta [1], Rücker et al. [2], Sakurai and Terui [3]). Hypoperfusion is a critical event in human brain with high risk of developing and functioning impairment. Hypoperfusion can induce vasomotion in ischaemia and sickle cell diseases (Hudetz et al. [4], Waltz et al. [5], Intaglietta [6]). In such situation, vasomotion may increase the blood flow by decreasing the effective vascular resistance (Meyer et al. [7]). The effective resistance during vasomotion would be the harmonic mean of the instantaneous resistance. This will differ in magnitude from the time average. The increased blood flow may lead to enhanced perfusion as reported by Sakurai and Terui [3]. According to them, tissue perfusion was 1.7 to 8.0 times larger than those without vasomotion. Therefore, one could assume that vasomotion is a regulating mechanism to control vascular resistance, blood flow and tissue perfusion.

Vasomotion is a local phenomenon which is observed both in the isolated arteries and in the intact animal such as humans, dogs, rabbits and rats (Kawasaki et al. [8], Gokina et al. [9], Omote et al. [10], Masuda et al. [11]). *In-vitro* experiments in isolated arteries denote that vasomotion is enhanced by vasoconstricting agonists such as noradrenaline (NE), acetylcholine (ACh), phenylephrine (PE), neuropeptide Y etc. Vasomotion is also noticed when the cells are depolarized with the help of

KCl solution (Dora et al. [12], Lamboley et al. [13], Seppely et al. [14], Peng et al. [15]).

At low dosages of agonists, ACh, NE, KCl, PE, either no vasomotion or vasomotion within only a small distance were reported (Lamboley et al. [13], Duling and Berne [16], Seppely et al. [14], Peng et al. [15]). However, at medium to high dosages, vasomotion was observed over the entire arteriole in the field of view. At very high concentration of NE, KCl and PE, tonic contraction was induced without calcium oscillations. Sufficient number of cells need to be stimulated at the same time to get vasomotion (Peng et al. [15]). These studies claim that minimum conditions are necessary for vasomotion to occur.

Spread of vasodilation is much faster than the movement of molecules by normal diffusion (Duling and Berne [16]). Diffusion of the substances through the gap junction is not the result of pure molecular diffusion but is a electro-diffusion transport. Vasomotion was disappeared when voltage was clamped in the Peng et al. [15] study. Vasomotion could be the result of faster cell to cell communication via ionic currents which in turn causes the change of calcium concentration in smooth muscle cells.

The need of mathematical models in vasomotion study was recognized very early by researchers and many mathematical models were developed (Goldbeter et al. [17], Gonzalez-Fernandez and Ermentrout [18], Parthimos et al. [19], Kapela et al. [20]). Koenigsberger et al. [21] assumed that calcium flux through gap junction is proportional to the difference in magnitude of calcium between the neighbouring cells. Same kind of equation is used to model voltage coupling. Voltage and calcium are separately coupled to their respective flux equations. Kapela et al. [22] used the Goldman-Hodgkin-Katz (GHK) equation to model the ionic currents through the gap junctions. This ionic currents were added to the membrane potential equation and corresponding ionic flux equations. Permeability was assumed to be the same for all ions. Gap junction resistance values available from experiments were used to calculate the permeability.

We aim to advance the mathematical modelling of vasomotion to explore the underlying mechanisms and the factors affecting the initiation and spread of vasomotion. In the present study, numerical analysis of minimal conditions required to initiate vasomotion is studied. A fixed length of artery with single layer SMCs are simulated with electro-diffusion coupling. Existing Gonzalez-Fernandez and Ermentrout [18] model with KCl induced stimulation is used in the simulations. Occurrence of conduction of contraction is analysed for different extracellular potassium concentrations, gap junction conductances and number of stimulated cells. The results are compared with

experimental results available.

### Mathematical Model

#### Single SMC

We have used Gonzalez-Fernandez and Ermentrout [18] model for simulating single cell dynamics. Inter-cellular ionic flux of calcium ion is added to this model equations to study multi-cell dynamics.

$$\frac{dn_i}{dt} = \lambda_n (n_\infty - n_i) \quad (1)$$

$$\frac{dv_{m,i}}{dt} = \frac{1}{C_m} [-g_L (v_{m,i} - v_L) - g_K n (v_{m,i} - v_{K,i}) - g_{Ca} m_\infty (v_{m,i} - v_{Ca,i}) - I_{gj,i}] \quad (2)$$

$$\frac{1}{\rho} \frac{d[Ca]_i}{dt} = -\alpha g_{Ca} m_\infty (v_{m,i} - v_{Ca,i}) - k_{Ca} [Ca]_i - \alpha I_{gj,i} \quad (3)$$

$$\frac{1}{\rho\alpha} \frac{d[Ca]_i}{dt} = C_m \frac{dv_{m,i}}{dt} + g_L (v_{m,i} - v_L) + g_K n (v_{m,i} - v_{K,i}) - \frac{k_{Ca} [Ca]_i}{\alpha} \quad (4)$$

$$m_{\infty,i} = 0.5 \left[ 1 + \tanh \frac{v_{m,i} - v_1}{v_2} \right] \quad (5)$$

$$n_{\infty,i} = 0.5 \left[ 1 + \tanh \frac{v_{m,i} - v_3}{v_4} \right] \quad (6)$$

$$v_{3,i} = -\frac{v_5}{2} \tanh \frac{Ca_i - Ca_3}{Ca_4} + v_6 \quad (7)$$

$$\lambda_{n,i} = \phi_n \cosh \frac{v_{m,i} - v_3}{2v_4} \quad (8)$$

$$v_{Ca,i} = \frac{RT}{Z_{Ca} F} \ln \left( \frac{[Ca]_e}{[Ca]_i} \right) \quad (9)$$

$$[Ca]_e = [Ca]_{in} \exp \left[ \frac{v_{Ca}^{base} Z_{Ca} F}{RT} \right] \quad (10)$$

$$v_{K,i} = \frac{RT}{Z_K F} \ln \left( \frac{[K]_{e,i}}{[K]_{in}} \right) \quad (11)$$

**Intercellular communication:** We have used the electro-diffusion coupling that suggested by Kapela et al. [22].

$$I_{gj,i} = \sum_j \frac{P Z_{Ca}^2 F^2}{RT} v_{gj} \left[ \frac{[Ca]_i - [Ca]_j \exp \left( \frac{-Z_{Ca} v_{gj} F}{RT} \right)}{1 - \exp \left( \frac{-Z_{Ca} v_{gj} F}{RT} \right)} \right] \quad (12)$$

$v_1$	-20.0 mV	Half-point of the calcium channel activation sigmoidal
$v_2$	25.0 mV	Slope of the calcium channel activation sigmoidal
$v_4$	14.5 mV	
$v_5$	8 mV	
$v_6$	-15.0 mV	
$g_L$	$7.854 \times 10^{-14} \text{ C s}^{-1} \text{ mV}^{-1}$	Whole cell leak conductance
$g_K$	$3.1416 \times 10^{-13} \text{ C s}^{-1} \text{ mV}^{-1}$	Whole cell potassium conductance
$g_{Ca}$	$1.57 \times 10^{-13} \text{ C s}^{-1} \text{ mV}^{-1}$	Whole cell calcium conductance
$Ca_3$	450.0 nM	
$Ca_4$	150.0 nM	
$C$	$1.9635 \times 10^{-14} \text{ C mV}^{-1}$	Cell capacitance
$K_d$	$1.0 \times 10^3 \text{ nM}$	Equilibrium constant of calcium and buffer reaction
$B_T$	$1.0 \times 10^5 \text{ nM}$	Total buffer concentration
$\alpha$	$7.9976 \times 10^{15} \text{ nM C}^{-1}$	
$\phi_n$	$2.664 \text{ s}^{-1}$	
$\beta$	$5.5 \times 10^{-1}$	Fraction of cell volume occupied by the cytosol
$v_L$	-70.0 mV	Nernst potential of leak
$v_{Ca}^{base}$	80.0 mV	Initial Nernst potential of calcium
$[Ca]_{in}$	70 nM	Initial intracellular Calcium concentration
$[K]_{in}$	140 mM	Intracellular potassium concentration
$k_{Ca}$	$1.3567537 \times 10^2 \text{ s}^{-1}$	Rate constant for cytosolic calcium extrusion
$R$	$8341.0 \text{ mJ mol}^{-1} \text{ K}^{-1}$	Universal gas constant
$T$	310.0 K	Temperature
$F$	$96487.0 \text{ C mol}^{-1}$	Faraday constant
$Z_{Ca}$	2	Valence of calcium ion
$Z_K$	2	Valence of potassium ion

$$v_{gj} = (v_{m,i} - v_{m,j}) \quad (13)$$

Where 'j' denotes neighbouring cells. This coupling term, equation 12, is added to the model equation for membrane voltage, equation 2. Corresponding calcium flux is obtained by multiplying equation 12 with  $\alpha$ . The resultant equation will be added to the differential equation of calcium, equation 3. Gap junctional conductance ( $G_{gj}$ ) of different connexin proteins is available in literature. It's value vary from 30 pS to 350 pS and is used to find the permeability of calcium ion through gap junction, equation 14.

$$P = \frac{RT G_{gj}}{F^2 Z_{Ca}^2} \frac{1}{[(Ca)_i + (Ca)_j] / 2} \quad (14)$$

**Cell stimulation:** KCl solution is widely used in *in-vitro* experiments to stimulate cells. In this study, extracellular potassium concentration, ( $[K]_e$ ), is changed to numerically simulate KCl induced cell dynamics [23]. Increasing extracellular potassium concentration will depolarize the cells to be stimulated and increases the opening of calcium channels.

**Numerical methods:** Model equations of calcium, membrane voltage and gating variable ( $n$ ) are discretized using backward Euler method. A coupled algorithm is used to solve resultant linear equations. This algorithm is similar to the one suggested by Rempe and Chopp [24]. For coupled cells, the system of linear equations will make a tridiagonal matrix which is solved by using Thomas algorithm.

#### Solution algorithm

- 1) Solve equation 2 and equation 1 at time  $t + \Delta t$  using values of  $[Ca]_i$ ,  $m_\infty$ ,  $v_3$ ,  $\lambda_n$ , and  $v_{Ca}$  at time  $t$
- 2) Recalculate fluxes using new values of  $n$  and  $v_{m,i}$
- 3) Solve equation 4 using updated fluxes,  $v_{m,i}$  and  $n$  at time  $t + \Delta t$
- 4) Calculate fluxes at time  $t + \Delta t$  using  $v_{m,i}$ ,  $[Ca]_{m,i}$  and  $n$  at time  $t + \Delta t$
- 5) got to step 1 untill the final time is reached

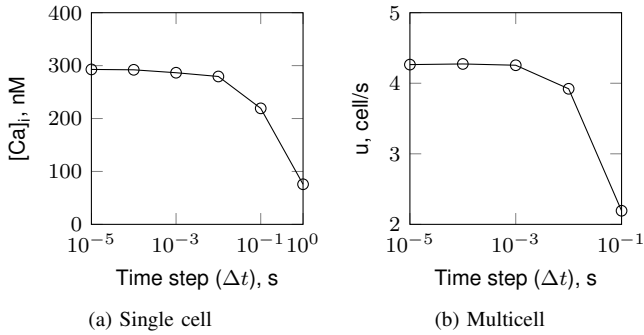


**Fig. 1: Solver dependency on time step:** (a) and (b) show variation of calcium concentration of single cell and propagation velocity of coupled cells respectively for different time steps

The dependency of time step on the single cell and multicell solvers are shown in the figures 1a and 1b. For single cell solver, converged results are obtained for  $\Delta t \leq 10^{-3}$ . To check the effect of additional gap junctional flux on the multicell solver, variation of propagation velocity against time step is analysed. It is clear from the figure 1b that propagation velocity is getting converged for  $\Delta t \leq 10^{-3}$ . We have used the time step of  $10^{-4}$  in all simulations to ensure accuracy in the results.

## II. RESULTS AND DISCUSSIONS

### Single cell dynamics

Figure 2 shows temporal changes of membrane potential in response to different extracellular potassium concentrations. As the extracellular potassium increase, the cell depolarizes into lower membrane potentials. Membrane voltage and calcium concentration start to oscillate when  $[K]_o > 4.2$  mM. Decrease of amplitude and increase of frequency is observed with respect to extracellular potassium concentration. However, the mean calcium concentration was increased to higher values. When  $[K]_o > 19.6$  mM, oscillation vanishes. The corresponding Hopf bifurcation diagram is given in the figure 2d.

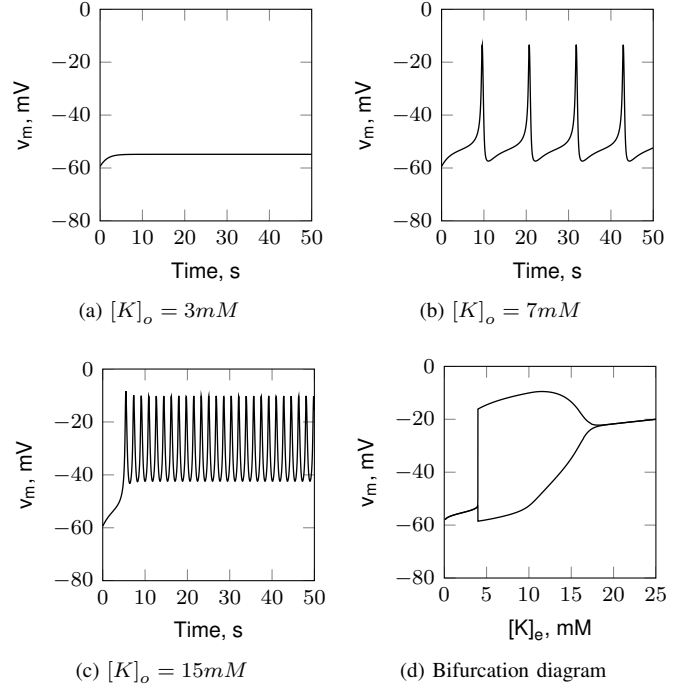


**Fig. 2: Membrane potential responses to extracellular potassium in single cell:**  $v_K$  is the Nernst potential of potassium ion for the corresponding extracellular potassium concentration.

### Multi-cell dynamics

Numerical simulations of single artery of mono-layer 1000 SMCs are conducted. One SMC will communicate with two adjacent SMCs. Vasomotion is generated by stimulating SMCs at the centre of the artery. Extracellular potassium concentration is varied from 3 mM to 50 mM. Extracellular potassium in the non-stimulating cells is kept at a normal level of 3.35 mM. This is approximately equal to -100 mV reverse potential of potassium. Stimulation of the cells are continued for 100 seconds and conduction of contraction is analysed.

**Minimal conditions for vasomotion:** Electro-diffusion of calcium ion through gap junction makes the conduction of contraction from the stimulated cells to the non-stimulated cells. Non-stimulated cell should receive net inflow of intercellular ionic current to depolarize itself. This means that the ionic current should be negative as shown in the figure 3. If the net inflow of intercellular ionic current is large enough to depolarize the adjacent non-stimulated cell, conduction occurs. The minimal conditions at which non-stimulated cells get depolarized are discussed below.

It is clear from the electro-diffusion equation, initial state of intercellular calcium flux from stimulated cell to non stimulated cell depends on the gap junctional conductance, gap junctional voltage and calcium differences. Voltage and calcium gradients can be controlled by changing extracellular potassium. In addition to that, number of stimulated cell on a specific length artery may also affect the conduction of contraction. The study of all these factors will help to define the minimal conditions required to occur vasomotion.

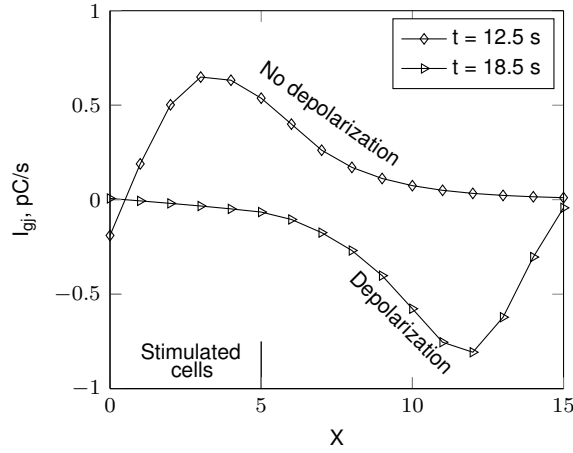


Fig. 3: Variation of intercellular ionic flux along the artery is plotted for two different time period. 10 cells at the center of the artery are stimulated using 8 mM extracellular potassium. Only first 15 cells on one half of the artery is shown here.  $G_{gj}$  is equal to 50 pS.

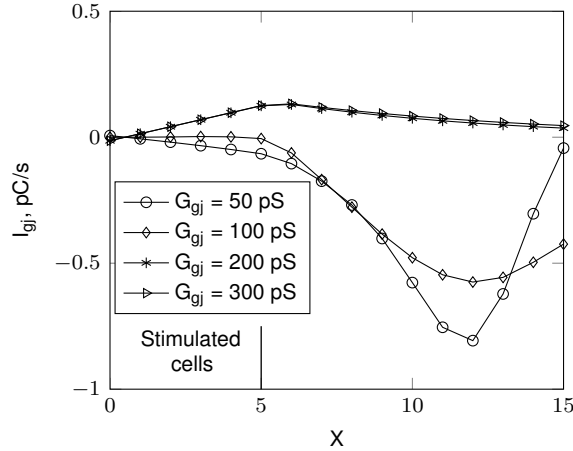


Fig. 4: Variation of intercellular ionic flux along the artery is plotted for different values of  $G_{gj}$ . 10 cells at the center of the artery are stimulated using 8 mM extracellular potassium. Only first 15 cells on one half of the artery is shown here. Corresponding time is equal to 18.5 seconds after stimulation started.

At high values of  $G_{gj}$ ,  $I_{gj}$  is always positive in all the cells, see figure 4. It means that no net inflow of intercellular ionic current is generated in non-stimulated cells to depolarize them. However, at small values of  $G_{gj}$ , initially positive  $I_{gj}$  is observed in non-stimulated cells. At certain time period after stimulation started, non-stimulated cells adjacent to stimulated cells receives net inflow of  $I_{gj}$  and get depolarized, see figure 4. If number of stimulated cells are kept constant, increasing gap junction conductance increases minimum amount of extracellular potassium required to initiate conduction, figure 5. The spatial distribution of current source may be increased to a far distance when  $G_{gj}$  is increased. In other words, source current will be distributed to more number of non-stimulated cells. This will reduce source current available to the non-

stimulated cell adjacent to the stimulated cell. To overcome this shortage, stimulated cells should be depolarized to higher values by increasing extracellular potassium. However, for  $G_{gj} > 500$  pS, minimum amount of extracellular potassium required is nearly constant. For smaller number of stimulated cells, constant region of extracellular potassium is obtained for less value of  $G_{gj}$ , figure 6. For  $N_{stim} \geq 15$ , required extracellular potassium is nearly the same for  $G_{gj} < 200$  pS, see figure 6.

Conduction starts to appear when  $[K]_e > 5$  mM. The

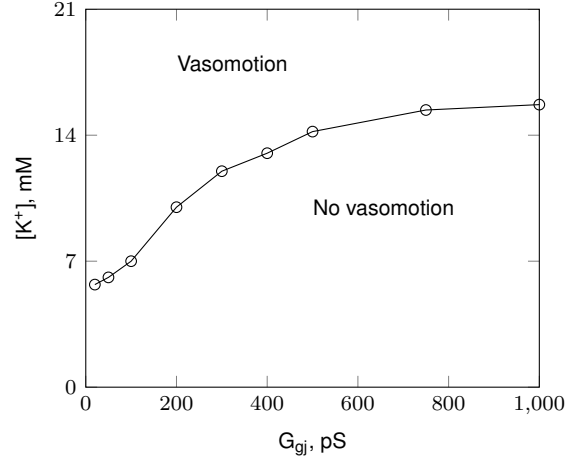


Fig. 5: Variation of minimum concentration of extracellular potassium over minimum  $G_{gj}$  at  $N_{stim} = 10$ .

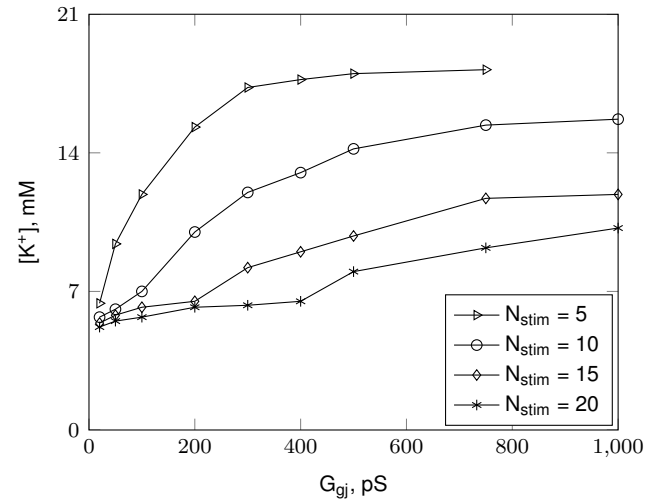


Fig. 6: Minimal conditions for initiating vasomotion for different number of stimulated cells

minimum number of cells needed to stimulate is not constant for all values of  $[K]_e$ . For  $[K]_e \geq 25$  mM, even a single cell stimulation can conduct vasomotion. But, when the  $[K]_e$  is reduced, the number of cells need to stimulate is increased. Around  $[K]_e = 6$  mM, small change in extracellular potassium can significantly change minimum number of stimulated cells required. It is evident from the figure 7 that that vasomotion only occurs if a minimal number of cells are depolarized by

sufficient amount of extracellular potassium. This is consistent with the experimental results of Peng et al. [15]. Minimum number of cells is not changing for increasing gap junctional conductance at high values of  $[K]_e$ , see figure 8. At low values of  $[K]_e$ , gap junctional conductance has significant influence on the occurrence of vasomotion.

For a constant extracellular potassium, more cells need to

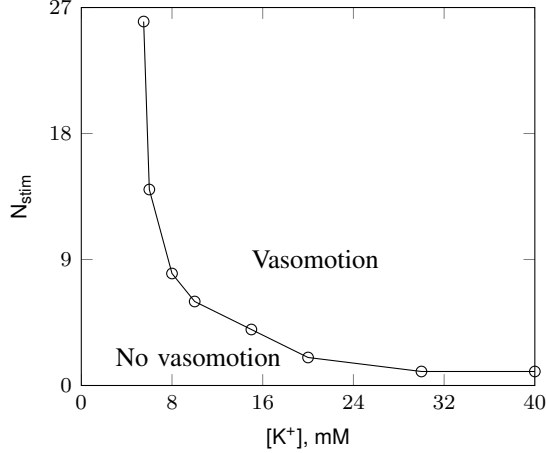


Fig. 7: Variation of minimum number of stimulated cells over minimum extracellular potassium at  $G_{gj} = 100$  pS

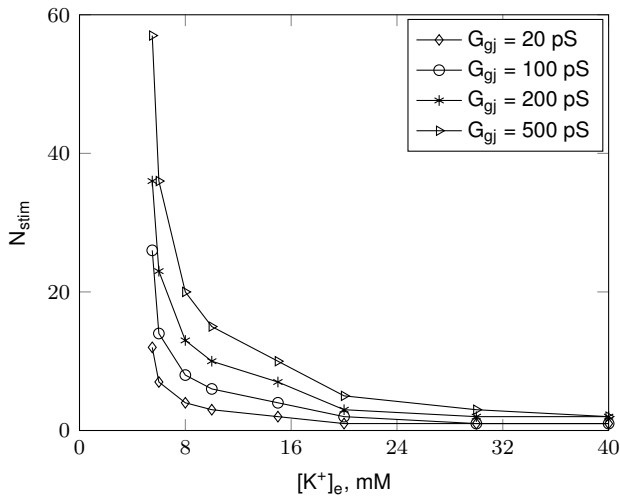


Fig. 8: Minimal conditions for initiating vasomotion for different  $G_{gj}$

be stimulated to initiate conduction when gap junction conductance is increased, figure 9. Increasing number of cells may expand source pool and keep enough transjunctional ionic flux to depolarize the adjacent non-stimulated cell. On the other hand, increasing  $G_{gj}$  may distribute the fixed source pool to more non-stimulated cells and reduce transjunctional ionic flux to the adjacent non-stimulated cell. Change in  $N_{stim}$  with respect to  $G_{gj}$  is large for small values of  $G_{gj}$ . This is accountable from the slope of the curve which increases at low values of  $G_{gj}$  and reaches a steady value when  $G_{gj}$  is greater than 500 pS. For different extracellular potassium

concentrations, figure 10, minimum  $N_{stim}$  is less influenced when  $G_{gj}$  is small.

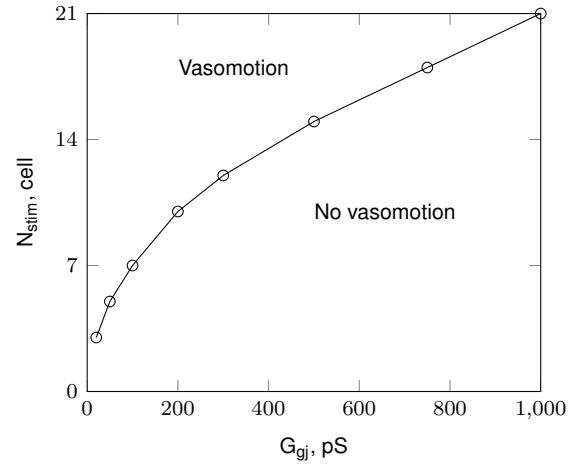


Fig. 9: Variation of minimum number of stimulated cells over minimum  $G_{gj}$  at  $[K^+]_e = 10$  mM

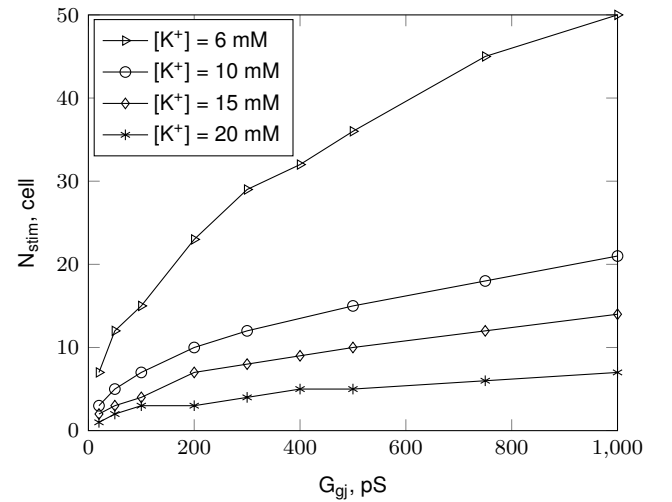


Fig. 10: Minimal conditions for initiating vasomotion for different extracellular potassium concentrations

*Model hypothesis:* We have adjusted Gonzalez-Fernandez and Ermentrout [18] model parameters to study KCl induced cell dynamics. Value of  $-v_1$  is fixed at -20.0 mV and extracellular potassium is varied to depolarize cell. Dynamic reverse potential of calcium ion is used instead of a constant value in the original model. Synchronization of calcium waves is necessary to get vasomotion in artery. This study is not focusing on that factor but was trying to understand the favourable conditions for conduction of cell depolarization towards non-stimulated cells. This is essential for occurring vasomotion.

Simulations are conducted only for fixed stimulation time and artery length. We have observed that time at which conduction occurs is not constant. If the stimulation keeps for longer time, conduction may appear in non-vasomotion region. Similarly

for artery length, changing length may change the minimum conditions of conduction. These factors will be taken care in future works.

### III. CONCLUSIONS

We have conducted numerical simulations to study the minimum conditions required to initiate vasomotion in single artery with a fixed length and fixed stimulation time. The main factors that affecting the conduction of contraction are strength of depolarization of the stimulated cells, number of cells stimulated and gap junction conductance. Influences of these factors on the presence of conducted contraction are analysed. Minimum number of cells need to stimulated for a fixed time period with a minimum amount of extracellular potassium and minimum intercellular conductance to depolarize non-stimulated cells and to occur vasomotion. This study help to understand favourable physical conditions for existence of vasomotion.

### ACKNOWLEDGMENT

The authors would like to thank...

### REFERENCES

- [1] A. G. Tsai and M. Intaglietta, "Evidence of flowmotion induced changes in local tissue oxygenation." *International journal of microcirculation clinical and experimental sponsored by the European Society for Microcirculation*, vol. 12, pp. 75–88, 1993.
- [2] M. Rücker, O. Strobel, B. Vollmar, F. Roesken, and M. D. Menger, "Vasomotion in critically perfused muscle protects adjacent tissues from capillary perfusion failure." *American journal of physiology. Heart and circulatory physiology*, vol. 279, pp. H550—H558, 2000.
- [3] T. Sakurai and N. Terui, "Effects of sympathetically induced vasomotion on tissue-capillary fluid exchange." *American journal of physiology. Heart and circulatory physiology*, vol. 291, no. 4, pp. H1761–H1767, Oct. 2006. [Online]. Available: <http://www.ncbi.nlm.nih.gov/pubmed/16731646>
- [4] A. Hudetz, B. Biswal, H. Shen, K. Lauer, and J. Kampine, "Spontaneous fluctuations in cerebral oxygen supply," in *Oxygen Transport to Tissue XX*, ser. Advances in Experimental Medicine and Biology, A. Hudetz and D. Bruley, Eds. Springer US, 1999, vol. 454, pp. 551–559. [Online]. Available: [http://dx.doi.org/10.1007/978-1-4615-4863-8\\_66](http://dx.doi.org/10.1007/978-1-4615-4863-8_66)
- [5] X. Waltz, A. Pichon, D. Mougenel, N. Lemonne, M. Lalanne-Mistrih, S. Sinnapah, V. Tarer, B. Tressières, Y. Lamarre, M. Etienne-Julan, O. Hue, M. Hardy-Dessources, and P. Connes, "Hemorheological alterations, decreased cerebral microvascular oxygenation and cerebral vasomotion compensation in sickle cell patients." *American journal of hematology*, vol. 87, no. 12, pp. 1070–1073, Dec. 2012. [Online]. Available: <http://www.ncbi.nlm.nih.gov/pubmed/22911571>
- [6] M. Intaglietta, "Arteriolar vasomotion: implications for tissue ischemia." *Blood Vessels*, vol. 28 Suppl 1, pp. 1–7, 1991.
- [7] C. Meyer, G. de Vries, S. T. Davidge, and D. C. Mayes, "Reassessing the mathematical modeling of the contribution of vasomotion to vascular resistance." *Journal of applied physiology (Bethesda, Md. : 1985)*, vol. 92, no. 2, pp. 888–9, Feb. 2002. [Online]. Available: <http://www.ncbi.nlm.nih.gov/pubmed/11838438>
- [8] K. Kawasaki, K. Seki, and S. Hosoda, "Spontaneous rhythmic contractions in isolated human coronary arteries." *Experientia*, vol. 37, no. 12, pp. 1291–1292, Dec. 1981. [Online]. Available: <http://www.ncbi.nlm.nih.gov/pubmed/7327230>
- [9] N. I. Gokina, R. D. Bevan, C. L. Walters, and J. A. Bevan, "Electrical Activity Underlying Rhythmic Contraction in Human Pial Arteries." *Circulation Research*, vol. 78, pp. 148–153, 1996. [Online]. Available: <http://circres.ahajournals.org/content/78/1/148.long>
- [10] M. Omote, N. Kajimoto, and H. Mizusawa, "The ionic mechanism of phenylephrine-induced rhythmic contractions in rabbit mesenteric arteries treated with ryanodine," *Acta Physiologica Scandinavica*, vol. 147, no. 1, pp. 9–13, 1993. [Online]. Available: <http://dx.doi.org/10.1111/j.1748-1716.1993.tb09467.x>
- [11] Y. Masuda, K. Okui, and Y. Fukuda, "Fine spontaneous contractions of the arterial wall of the rat in vitro." *Japanese Journal of Physiology*, vol. 32, pp. 453–457, 1982.
- [12] K. A. Dora, J. Xia, and B. R. Duling, "Endothelial cell signaling during conducted vasomotor responses." *American journal of physiology. Heart and circulatory physiology*, vol. 285, no. 1, pp. H119–H126, Jul. 2003. [Online]. Available: <http://www.ncbi.nlm.nih.gov/pubmed/12793976>
- [13] M. Lamboley, A. Schuster, J. Bény, and J. Meister, "Recruitment of smooth muscle cells and arterial vasomotion." *American journal of physiology. Heart and circulatory physiology*, vol. 285, no. 2, pp. H562–9, Aug. 2003. [Online]. Available: <http://www.ncbi.nlm.nih.gov/pubmed/12574002>
- [14] D. Seppey, R. Sauser, M. Koenigsberger, J. Bény, and J. Meister, "Intercellular calcium waves are associated with the propagation of vasomotion along arterial strips." *American journal of physiology. Heart and circulatory physiology*, vol. 298, no. 2, pp. H488–96, Feb. 2010. [Online]. Available: <http://www.ncbi.nlm.nih.gov/pubmed/19966061>
- [15] H. Peng, V. Matchkov, A. Ivarsen, C. Aalkjar, and H. Nilsson, "Hypothesis for the Initiation of Vasomotion," *Circulation Research*, vol. 88, no. 8, pp. 810–815, Apr. 2001. [Online]. Available: <http://circres.ahajournals.org/cgi/doi/10.1161/hh0801.089603>
- [16] B. R. Duling and R. M. Berne, "Propagated Vasodilation in the Microcirculation of the Hamster Cheek Pouch," *Circulation Research*, vol. 26, no. 2, pp. 163–170, Feb. 1970. [Online]. Available: <http://circres.ahajournals.org/cgi/doi/10.1161/01.RES.26.2.163>
- [17] A. Goldbeter, G. Dupont, and M. J. Berridge, "Minimal model for signal-induced Ca<sup>2+</sup> oscillations and for their frequency encoding through protein phosphorylation." *Proceedings of the National Academy of Sciences of the United States of America*, vol. 87, no. 4, pp. 1461–5, Feb. 1990. [Online]. Available: <http://www.pubmedcentral.nih.gov/articlerender.fcgi?artid=53495&tool=pmcentrez&rendertype=abstract>
- [18] J. M. Gonzalez-Fernandez and B. Ermentrout, "On the

- origin and dynamics of the vasomotion of small arteries.” *Mathematical Biosciences*, vol. 119, pp. 127–167, 1994.
- [19] D. Parthimos, D. H. Edwards, and T. M. Griffith, “Minimal model of arterial chaos generated by coupled intracellular and membrane  $\text{Ca}^{2+}$  oscillators,” *American journal of physiology. Heart and circulatory physiology*, vol. 277, pp. H1119–H1144, 1999.
  - [20] A. Kapela, A. Bezerianos, and N. M. Tsoukias, “A mathematical model of  $\text{Ca}^{2+}$  dynamics in rat mesenteric smooth muscle cell: agonist and NO stimulation.” *Journal of theoretical biology*, vol. 253, no. 2, pp. 238–260, Jul. 2008. [Online]. Available: <http://www.ncbi.nlm.nih.gov/pubmed/18423672>
  - [21] M. Koenigsberger, R. Sauser, M. Lambole, J.-L. Béný, and J. Meister, “ $\text{Ca}^{2+}$  dynamics in a population of smooth muscle cells: modeling the recruitment and synchronization.” *Biophysical journal*, vol. 87, no. 1, pp. 92–104, Jul. 2004. [Online]. Available: <http://www.pubmedcentral.nih.gov/articlerender.fcgi?artid=1304399&tool=pmcentrez&rendertype=abstract>
  - [22] A. Kapela, S. Nagaraja, and N. M. Tsoukias, “A mathematical model of vasoreactivity in rat mesenteric arterioles. II. Conducted vasoreactivity.” *American journal of physiology. Heart and circulatory physiology*, vol. 298, no. 1, pp. H52–H65, Jan. 2010. [Online]. Available: <http://www.pubmedcentral.nih.gov/articlerender.fcgi?artid=2806131&tool=pmcentrez&rendertype=abstract>
  - [23] M. Koenigsberger, R. Sauser, J. Béný, and J. Meister, “Effects of arterial wall stress on vasomotion.” *Biophysical journal*, vol. 91, no. 5, pp. 1663–1674, Sep. 2006. [Online]. Available: <http://www.pubmedcentral.nih.gov/articlerender.fcgi?artid=1544282&tool=pmcentrez&rendertype=abstract>
  - [24] M. J. Rempe and D. L. Chopp, “A predictor-corrector algorithm for reaction-diffusion equations associated with neural activity on branched,” *SIAM Journal of Scientific computing*, vol. 28, no. 6, pp. 2139–2161, 2006.